INNOVATIVE AIRCRAFT HEAT EXCHANGER INTEGRATION FOR HYDROGEN-ELECTRIC PROPULSION

M. Ronovsky-Bodisch*, B. Gerl*, M. Berens*

* Technische Universität Wien, Forschungsgruppe Luftfahrzeugsysteme, Lehargasse 6, 1060 Wien, Österreich

Abstract

Propulsion systems in aircraft that use reciprocating engines often face the challenge of managing thermal loads effectively. This problem is very similar to the usage of PEM fuel cell systems, which despite their very high efficiency generate a high proportion of heat when converting fuel energy into electrical energy. To address this, the integration of heat exchangers into the propulsion architecture offers the dual benefit of dissipating excess heat and harnessing it for additional thrust generation through the ram jet effect. Striving for enhanced thrust performance, this paper presents different parameters (operating conditions, FPR, diffusion ratio, air side temperature difference) and their influence. Based on an 1D-modelling approach the challenges and possibilities of combining a thrust generation system with a heat exchanger are discussed.

Keywords

Hydrogen electric propulsion; Fuel Cell Cooling; Heat recovery

NOMENCLATURE

Symbols

A	Area	m^2
A_{15}/A_1	Ratio of HX air inlet to fan inlet areas	
A_{HX}	Heat exchanger surface area	m^2
α_{air}	Air Heat transfer coefficient	$W/(K\ m^2)$
b_{triang}	Side length of HX air flow channel	mm
c_p	Specific heat capacity	J/(kg K)
Δp_{HX}	HX pressure loss	Pa
ΔT_{ISA}	ISA temperature deviation	K
ΔT_{liq}	ΔT coolant in- and outflow	K
ΔT_w	ΔT coolant and air side wall	K
d_h	Hydraulic diameter	m
$\eta_{f,poly}$	Fan polytropic efficiency	
η_{fcs}	Fuel cell system efficiency	
η_{tot}	Total efficiency	
η_{trans}	Transfer efficiency	
F	Thrust	N
$FNPR$	Fan nozzle pressure ratio	
FPR	Fan pressure ratio	
γ	Heat capacity ratio	
H	Flight altitude	ft
h_{HX}	Lenght of the HX	m
k_d	Roughness height	µm
λ_{air}	Air heat conductivity	W/(K m)
λ_{pl}	Friction factor	
$\dot{m}$	Air mass flow	kg/s
M_0	Freestream Mach number	
M_1	Fan inlet Mach number	
$No_{ch,air}$	Number of HX air side channels	
$Nu_{m,air}$	Heat exchanger average Nusselt number	
p	Static Pressure	Pa
P_{av}	Propulsive power	W
P_{br}	Power at fan shaft	W
P_{fuel}	Fuel Power	W
$P_{kin,j}$	Jet kinetic power	W
PR	Ratio of total to static pressure	
PR_{crit}	Critical nozzle pressure ratio	
p_{tot}	Total pressure	Pa
$\dot{Q}_{FC}$	Assumed heat to be rejected	W
q_{HX}	HX air side dynamic pressure	Pa
Re	Reynolds number	

ρ	Density	kg/m^3
T	Static temperature	K
$T_{\text{in,liq}}$	Coolant inflow temperature	°C
$T_{\text{tot,m,air}}$	HX average total air temperature	K
T_{tot}	Total temperature	K
$T_{\text{w,m,air}}$	HX average wall temperature	K
U	Circumferential length of HX air channel	m
V	Air flow velocity	m/s
V_{j}	Fully expanded jet velocity	m/s

Indices

0	Freestream
1	Fan
15	Upstream of heat exchanger
19	Nozzle exit

1. INTRODUCTION

To achieve fully electric flight, hydrogen fuel cell propulsion systems are considered a promising option. In contrast to gas turbines the energy conversion in fuel cells does not allow for the heat removal with the exhaust gases. Therefore fuel cells require thermal management systems (TMS) to efficiently dissipate heat to the environment [1], resulting in increased system mass and additional drag. Various designs are possible for heat transfer to the surroundings. The heat can be dissipated convectively via surface coolers, by convection and/or radiation, or by means of air-flow heat exchangers. The latter method is discussed in this paper. This is especially a problem for low temperature polymer electrolyte membrane fuel cells (LT-PEMFC), which are - due to their comparatively high TRL - considered in this study as well as in most contemporary hydrogen fuel cell aircraft designs, even though other fuel cell types are in development for aviation. LT-PEMFC have a peak electrical efficiency of 50 – 60% based on the lower heating value of hydrogen. Operating temperatures are low around 80°C [2]. Therefore large air side heat exchange (HX) surface areas are required for convective dissipation of so-called "low quality" heat. This is especially problematic considering hot day take-off scenarios with low temperature difference between coolant and ambient air. The large heat exchanger surface area results in high air side pressure losses. Design concepts for heat exchanger installations aim for heat dissipation with minimal pressure losses. This can be achieved by flow velocity reduction in a specially designed air duct [3]. Becker and Baals [4] investigated the effects of drag reduction using the ram jet effect by combining the heat exchanger with an air duct consisting of diffuser and nozzle. Making use of the ram jet effect does not only allow for drag reduction but can bring the advantage of additional thrust generation, if pressure losses within the HX are low enough.

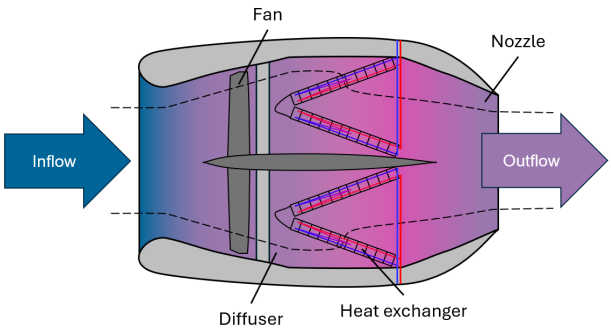

FIG. 1. Schematic layout of the heat propulsor

This paper investigates the combination of the heat exchanger and the propulsion system for the dual benefit of dissipating excess heat and harnessing it for additional thrust generation due to the ram jet effect. The combination is called "heat propulsor" and consists of a ducted propulsor with the heat exchanger located between fan stage and variable area nozzle, see Fig. 1. The addition of the fan stage in front of the heat exchanger is beneficial, because the efficiency of the Brayton cycle, which is the underlying process of the ram jet effect, improves with increasing pressure. Showing different parameters and their influence this paper strives to present the challenges and possibilities of combining the thrust generation system with the HX, based on an 1D-modelling approach.

2. MATERIAL AND METHOD

In order to design the heat propulsor, a fundamental understanding on the influence of different operating conditions and parameters must be gained. The size of the heat exchanger influences the pressure losses and as a result the additional thrust gained. The frontal surface area of the heat exchanger (A_{15}) defines the diffusion ratio and its length influences the pressure losses. It is important to note that Fig. 1 and Fig. 2 depict the heat propulsor differently: Fig. 1 shows an oblique configuration, while Fig. 2 illustrates an installation with the inlet area perpendicular to the airflow. From a design point of view an oblique heat exchanger installation offers the benefit of increased flow area and hence lower flow velocities while maintaining the external diameter of the duct. The effects of heat exchanger frontal surface area and flow channel inclination on pressure losses and heat transfer coefficient are outlined in [5]. Since the influence of the change in flow direction on the pressure losses is very complex and cannot be adequately modelled with the selected model accuracy, the inclined position of the heat exchanger is not taken into account. Thus on a fluid dynamic level the air flow conditions are calculated as if the heat exchanger surface area is perpendicular to the flow direction, Fig. 2, even though the oblique installation in Fig. 1 is assumed.

The necessary heat exchanger size is dependent on different parameters and varies significantly between take-off

and cruise. Thus the calculation is not based on a set heat exchanger surface area; instead the whole engine is rubberized and scaled according to the specified parameters. The only fixed geometry parameter is the area ratio of the diffuser A_{15}/A_1, see Fig. 1. The frontal surface area of the fan (A_1), heat exchanger surface area and the nozzle outlet area are calculated depending on the input parameters. The heat propulsor is sized to fulfill a specified net thrust demand, which includes the additional thrust due to the ram jet effect. Not considered, however, is the external nacelle drag which is influenced by system size.

2.1. Air duct

The calculation of the air duct assumes one dimensional flow with constant velocity distribution over the entire cross section. All internal losses in the air duct are neglected, assuming they are much smaller in comparison to the pressure losses occurring in the heat exchanger. Even though it might prove beneficial to combine the intake and outlet for the air supply of the fuel cell and the environmental control system (ECS) with the heat propulsor, no air mass flow is diverted or added for other theoretical system components. Thus mass flow in the air duct is constant.
For the flow conditions of the freestream far ahead of the air duct the Mach number is specified and environment conditions according to the international standard atmosphere (ISA) [6] dependent on the altitude are set. To simulate different environment conditions deviating from ISA, a temperature difference can be specified. No detailed modelling of the air intake is done; it is assumed that the air inlet is designed to provide a specified Mach number M_1 at the fan face. The design of a suitable air inlet for fuel cell aircraft TMS is a challenging task balancing complexity and mass [7]. A fan stage polytropic efficiency independent of the fan pressure ratio (FPR) is taken into account. Station 15 describes the operating conditions right in front of the heat exchanger, see Fig. 2, based on the following equations:

$$FPR = \frac{p_{\text{tot,15}}}{p_{\text{tot,0}}} \tag{1}$$

$$\frac{T_{\text{tot,15}}}{T_0} = FPR^{\frac{\gamma-1}{\eta_{\text{f,poly}}\gamma}} \tag{2}$$

After the fan stage follows the heat exchanger; this stage will be described in further detail in the next section. Because the losses in the air duct are neglected, the total pressure at the heat exchanger outlet is identical to the total pressure at the nozzle outlet (station 19). The nozzle exit area A_{19} is determined according to the necessary mass flow to achieve the set thrust demand using Eq. (3) – (9).

$$F_{\text{net}} = \dot{m} \cdot (V_{\text{j}} - V_0) + A_{19} \cdot (p_{19} - p_0) \tag{3}$$

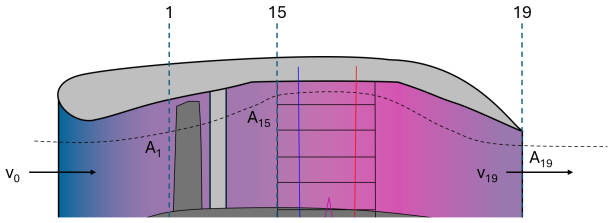

FIG. 2. Numbering of the heat propulsor stages

$$FNPR = \frac{p_{\text{tot,19}}}{p_{19}} \tag{4}$$

$$FNPR = FPR \cdot \frac{1 + \frac{\Delta p_{\text{HX}}}{p_{\text{tot,19}}}}{\frac{p_{\text{tot,0}}}{p_{19}}} \tag{5}$$

$$V_{\text{j}} = \sqrt{\frac{2\gamma R\, T_{\text{tot,19}}}{\gamma - 1}\left(1 - FNPR^{\frac{1-\gamma}{\gamma}}\right)} \tag{6}$$

$$MFP_{\text{i}} = \sqrt{\frac{2\gamma}{R(\gamma-1)}} \frac{1}{PR_{\text{i}}^{\frac{1}{\gamma}}} \sqrt{1 - \frac{1}{PR_{\text{i}}^{\frac{\gamma-1}{\gamma}}}} \tag{7}$$

$$\frac{\dot{m}}{A_{\text{i}}} = MFP_{\text{i}} \cdot \frac{P_{\text{tot,i}}}{\sqrt{T_{\text{tot,i}}}} \tag{8}$$

$$\frac{A_{19}}{A_1} = \frac{\frac{\dot{m}}{A_1}}{\frac{\dot{m}}{A_{19}}} \tag{9}$$

Note that in case nozzle choking the nozzle static pressure p_{19} is no longer equal to the ambient static pressure p_0 and needs to be calculated using the critical pressure ratio PR_{crit}. Eq. (3) – (9) can be used for both a choked and unchoked nozzle.

2.2. Heat exchanger

A counter flow compact plate fin heat exchanger is modelled in the calculation based on a simple 1D-modelling approach, which was chosen as a simplification. In practical application, however, the heat exchanger is most likely in a cross-flow design. The heat exchanger consists of equilateral triangular air flow channels, see Fig. 3, whose number is dependent on the set side length of an individual air channel and the frontal surface area of the HX. For the HX geometry the coolant flow channels as well as the wall thickness are neglected. Nevertheless the coolant mass flow is calculated based on single pass coolant channels and a constant temperature difference between coolant and wall (air side) is estimated. Based on these assumptions the required heat exchanger surface area A_{HX} and length h_{HX} are calculated depending on the operating conditions.

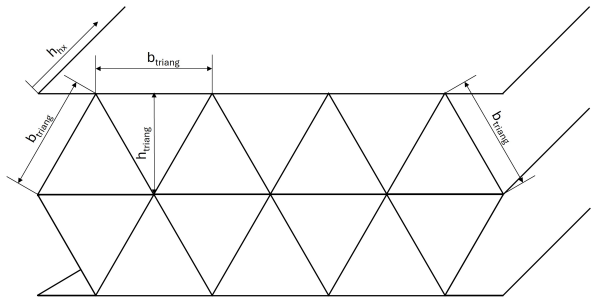

FIG. 3. Sketch of the heat exchanger geometry

Parameter	Value
ISA temperature deviation ΔT_{ISA} (K)	0
Fuel cell system efficiency η_{fcs}	0.5
Fan polytropic efficiency $\eta_{\mathsf{f,poly}}$	0.85
Fan pressure ratio FPR	1.2 – 1.6
Fan inlet Mach numberM_1	0.5
Side length of HX air flow channel b_{triang} (mm)	10
ΔT coolant and air side wall ΔT_{w} (K)	5
Roughness height $k_{\mathsf{d}}(\mu\mathrm{m})$	0

TAB. 1. Constant input parameters

$$\alpha_{\mathsf{air}} = \frac{Nu_{\mathsf{m,air}}\lambda_{\mathsf{air}}}{d_{\mathsf{h}}} \tag{10}$$

$$A_{\mathsf{HX}} = \frac{\dot{Q}_{\mathsf{FC}}}{\alpha_{\mathsf{air}} \cdot (T_{\mathsf{w,m,air}} - T_{\mathsf{tot,m,air}})} \tag{11}$$

$$h_{\mathsf{HX}} = \frac{A_{\mathsf{HX}}}{UNo_{\mathsf{ch,air}}} \tag{12}$$

The amount of heat that needs to be transferred depends on the compression power of the fan required for a given thrust demand. Other heat sources, like the electric motors, transmission or batteries, are not included at this stage. Future concepts might try to include multiple heat sources at different temperature levels. To better analyse the effect of altitude on the heat propulsor, the fuel cell system efficiency is constant and independent of the operating conditions.

$$\dot{Q}_{\mathsf{FC}} = (\frac{1}{\eta_{\mathsf{fcs}}} - 1) \cdot c_{\mathsf{p}}\dot{m} \cdot (T_{\mathsf{tot,15}} - T_{\mathsf{tot,0}}) \tag{13}$$

The flow within the air channels is assumed to be fully turbulent, neglecting the flow development at the air channel inlets [8]. Thus the air channel size is chosen to ensure a Reynolds number above 4000. For the pressure losses of turbulent flow the friction factor λ_{pl} according to Zanke is used, allowing for the calculation of hydraulically smooth and rough channels [9].

$$q_{\mathsf{HX}} = \frac{1}{2} \cdot \rho_{\mathsf{m,air}} V^2_{\mathsf{m,air}} \tag{14}$$

$$\Delta p_{\mathsf{HX}} = q_{\mathsf{HX}}\ \lambda_{\mathsf{pl}}(Re)\ \frac{h_{\mathsf{HX}}}{d_{\mathsf{h}}} \tag{15}$$

Because the flow conditions at the heat exchanger exit cannot be directly calculated an iteration loop is used to determine the size of the heat propulsor as well as the required mass flow.

3. RESULTS AND DISCUSSION

The parameter study is divided into three sections. First the influence of altitude on the heat propulsor efficiency will be discussed to show the optimal operating point of the heat propulsor. Thereafter the pressure losses will be discussed followed by the effects of different parameters on the geometry. For this parameter study existing aircraft of mega-watt class in the short to medium range (SMR) segment, like the Airbus A320, are considered as a reference. Conventional fuel cell powered aircraft designs are based on propeller configurations. Because the investigated heat propulsor is a combination of a ducted propulsor or impeller concept combined with a heat exchanger, see Fig. 1, turbofan rather than turboprop aircraft are used as a reference. At this point should be mentioned that the goal of the heat propulsor developed in the exFan-Project is not to reengine existing aircraft and that the final integration concept does not have to be a conventional underwing nacelle configuration. The input parameters, which remain unchanged throughout the three parameter studies, are stated in Tab. 1; net thrust demand, cruise Mach number and flight altitude are based on SMR sized aircraft. Changes in fuel cell system efficiency and fan polytropic efficiency dependent on the operating conditions are neglected.

3.1. Performance investigation

To understand why the proposed propulsion system deviates from conventional fuel cell aircraft concepts, the influence of flight altitude on the efficiencies must be taken into account. In this study the net thrust and flight Mach number are constant and only the flight altitude is varied between 8000m and 15000m for different fan pressure ratios, see Tab. 2. Further, the benefit of the combined propulsion and heat rejection system is shown.

3.1.1. Optimal operating point

The heat propulsor performs best at high Mach numbers, because the higher dynamic pressure increases the efficiency of the ram jet effect. Also the flight altitude has an influence on the heat propulsor efficiency. The transfer efficiency is defined as the ratio of kinetic jet power to the power added by the fan and includes the fan and heat exchanger losses as well as the effects of the ram jet. Because further energy is added to the air flow by the heat exchanger, the transfer efficiency can be greater than one if the ram jet effect compensates the

Parameter	Value
Flight altitude H (km)	8 – 15
Freestream Mach number M_0	0.78
Net Thrust F_{net} (kN)	23.020
Coolant inflow temperature $T_{\text{in,liq}}$ (°C)	80
ΔT coolant in- and outflow ΔT_{liq} (K)	10
Ratio HX air inlet to fan inlet areas A_{15}/A_1	3

TAB. 2. Parameters used for performance investigation

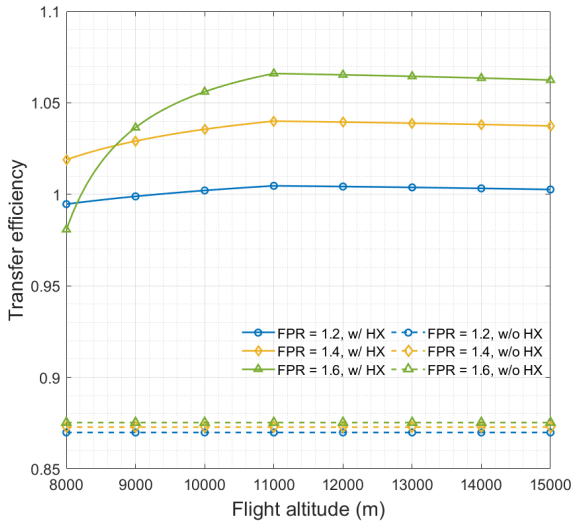

FIG. 4. Comparison of transfer efficiency over flight altitude

fan and HX losses.

$$\eta_{\text{trans}} = \frac{P_{\text{kin,j}}}{P_{\text{br}}} = \frac{\text{Kinetic jet power}}{\text{Power at fan shaft}} \tag{16}$$

Comparing the transfer efficiency for different altitudes in Fig. 4 shows that the best performance is achieved at 11km. According to the international standard atmosphere (ISA) [6] ambient temperature and pressure decrease between sea level and the tropopause at 11km. The decreasing ambient temperature results in higher temperature difference in the heat exchanger, which reduces the required heat transfer surface area. A small heat transfer surface area is beneficial, because it reduces the air side pressure losses. Above 11km the ambient temperature is constant and only the pressure decreases further. Thus the HX surface area does no longer decrease with altitude due to no more reduction in HX air temperature difference and instead it slowly increases again. In summary the best operating point for the heat propulsor to gain the highest benefit from the ram jet effect is close to the tropopause at 11km. To ensure that the energy required to reach such altitudes is worthwhile and that the Meredith effect can be utilised as effectively as possible, the propulsion system is better suited for SMR aircraft than for regional aircraft.

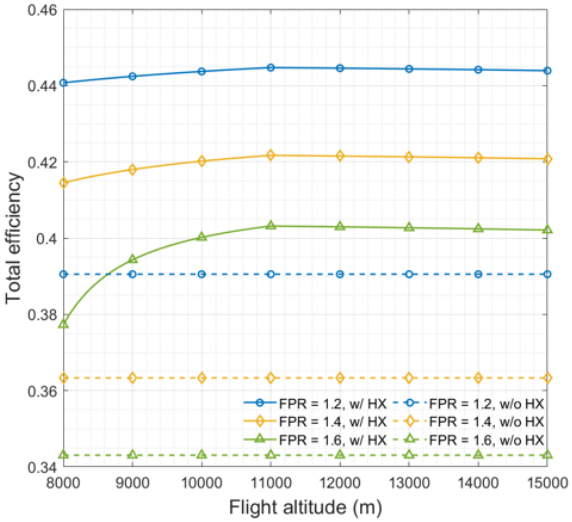

FIG. 5. Comparison of total efficiency over flight altitude

The optimal operating point is also shown for the total efficiency in Fig. 5. Note that the efficiency of the fuel cell system is assumed to be independent of altitude. In reality, however, the efficiency would decrease due to higher compression power of the air supply system. This would shift the total efficiency to lower values.

$$\eta_{\text{tot}} = \frac{P_{\text{av}}}{P_{\text{fuel}}} = \frac{\text{Propulsive power}}{\text{Fuel power}} \tag{17}$$

Comparing transfer efficiency and total efficiency (Fig. 4 and Fig. 5) shows that for greater FPRs the transfer efficiency is higher while the total efficiency is lower. This is due to the jet efficiency (ratio of kinetic power at the nozzle to the actual propulsive power) being higher at lower pressure levels. As a result low FPRs have a positive impact on the performance of the heat propulsor, which will also be shown in the following section in terms of heat exchanger geometry.

3.1.2. Comparison to non recuperating propulsors

Fig. 4 and Fig. 5 further compare the heat propulsor to a non recuperating fuel cell propulsion system. As a reference serves a ducted propulsor with a separate heat exchanger system for the fuel cell. The means of heat dissipation is not specified; the heat exchanger system is assumed as a "notional surface cooler". The drag induced by this unspecified heat exchanger configuration is neglected.

The comparison of the two systems shows that making use of the ram jet effect brings a significant advantage for the performance of a fuel cell aircraft. At the optimal operating point the heat propulsor provides a net gain of 5.4% total efficiency (at FPR 1.2). The increase in air temperature due to the compression in the fan stage results in a larger heat exchanger. However, this disadvantage is overcome, because the drag induced by the heat exchanger compensated and additional thrust is generated. Thus the proposed configuration brings sig-

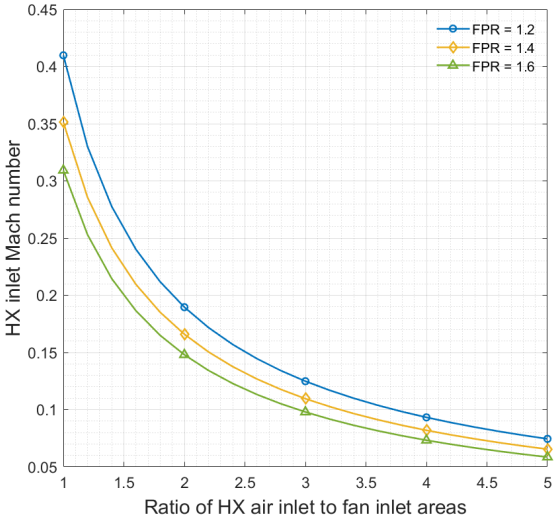

FIG. 6. Impact of diffusion ratio on HX inlet Mach number

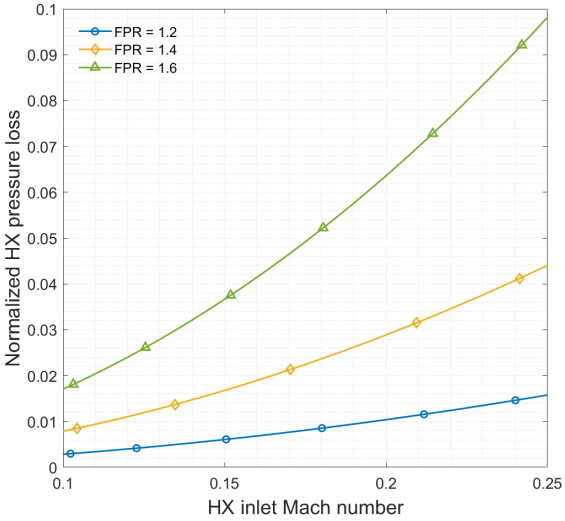

FIG. 7. Impact of HX inlet Mach number on pressure losses

Parameter	Value
Flight altitude H (ft)	35000
Freestream Mach number M_0	0.78
Net Thrust F_{net} (kN)	23.020
Coolant inflow temperature $T_{\text{in,liq}}$ (°C)	80
Ratio of HX air inlet to fan inlet areas A_{15}/A_1	1 – 5

TAB. 3. Parameters used for pressure loss investigation

Parameter	Take-off	Cruise
Flight altitude H (ft)	0	35000
Freestream Mach number M_0	0.22	0.78
Net Thrust F_{net} (kN)	120.143	23.020
Ratio of HX air inlet to fan inlet areas A_{15}/A_1	3 or 1 – 5	
Coolant inflow temperature $T_{\text{in,liq}}$ (°C)	80 or 80 – 140	

TAB. 4. Parameters used for geometry investigation

nificant advantages during cruise compared to other heat exchanger integrations.

3.2. Pressure loss investigation

The pressure losses in the heat exchanger represent the major loss within the heat propulsor - if they are to big no additional thrust can be gained. The pressure losses are determined by the air flow velocity and the length of the heat exchanger. To reduce the air flow velocity as much as possible high diffusion ratios are required, see Fig. 6. Because the diffusion ratio is defined by the ratio of heat exchanger frontal area to fan area, conventional diffuser designs would lead to large cross sections in the heat propulsor. Thus the necessity of oblique heat exchanger configurations arises. As a drawback the change in flow direction leads to increasing pressure losses, requiring an efficient design for the integration of the heat exchanger into the air duct [10,11]. As this topic exceeds the scope of the present study, future investigations will focus on CFD simulations.

Low flow velocities reduce the pressure losses in the heat exchanger as shown in Fig. 7, where the heat exchanger inlet Mach number is plotted against the normalized pressure losses, see Eq (18). Especially for higher FPRs the HX inlet Mach number has a strong influence on the pressure losses. This is due to the fact, that higher FPRs require greater compression power and therefore higher amounts of heat need to be dissipated from the fuel cell. The resulting growth in the length of the heat exchanger increases pressure losses.

$$\frac{\Delta p_{\text{HX}}}{p_{\text{tot,15}}} = \frac{p_{\text{tot,15}} - p_{\text{tot,19}}}{p_{\text{tot,15}}} \tag{18}$$

3.3. Geometry investigation

This section is focused on the influence of fan pressure ratio, coolant temperature and the diffusion ratio on the heat propulsor geometry to show the trade-off between performance and size. Further the take-off problem is discussed, which arises from strongly deviating ambient conditions and power requirements between take-off and cruise resulting in a significant difference in heat exchanger surface area. Only these two flight scenarios are analysed in this section. The take-off and cruise scenarios differ only in Mach number, altitude (defines the ambient conditions) and net thrust; all other parameters remain unchanged, see Tab. 1 and Tab. 4

3.3.1. Heat exchanger surface area

The low coolant temperature of LT-PEM fuel cells poses a major challenge for the cooling system due to the low heat quality. This leads to large heat exchanger surface areas, particularly during hot day take-off scenarios, because the low temperature difference is combined with high power demand. During cruise flight, however, the required heat exchanger area is smaller (higher temperature difference, lower power requirement). Due to the different demands on the heat exchanger over the flight mission and the strong influence of the heat exchanger on the additional thrust gain of the heat propulsor, this study pays particular attention to the heat exchanger surface and length.

As discussed above, a higher diffusion ratio reduces the air flow velocity lowering pressure losses, but at the same time the heat transfer coefficient deceases as well. This results in a higher required heat exchanger surface area. Fig. 8 shows the influence of diffusion ratio on the heat exchanger size for different fan pressure ratios. In conclusion the reduction in pressure loss due to lower flow velocities has the drawback of higher heat exchanger mass and volume.

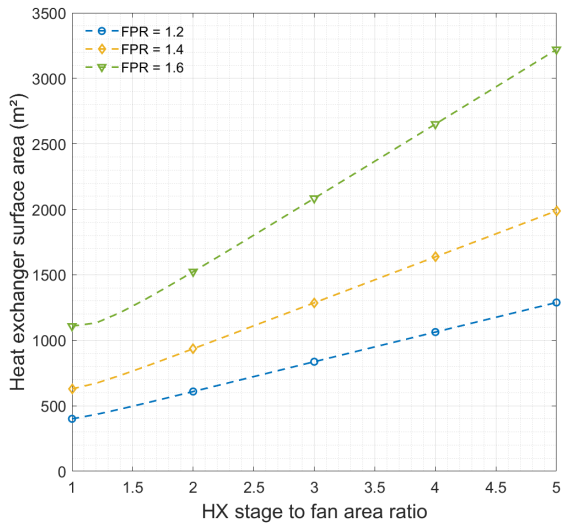

FIG. 8. Influence of area ratio on heat exchanger surface area

Fig. 9 shows the heat exchanger surface area during both load cases at ISA environment conditions. As discussed before a higher FPR increases the HX surface area. This is on one part due to the higher amount of heat, because the fuel cell power increases with FPR. For the other part the total temperature upstream of the heat exchanger increase with higher compression ratios, further decreasing the temperature difference in the HX, see Eq. (2).

The coolant temperature has a strong influence on the surface area, because a higher temperature difference improves the HX performance and thereby reduces size, see Fig. 9. During cruise a higher coolant temperature has a lesser impact on performance due to reduction in pressure losses. However, the influence of the coolant temperature is of major importance during take-off. To achieve a

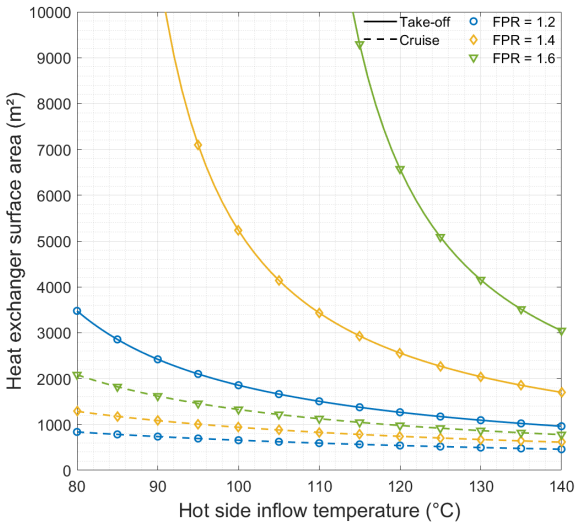

FIG. 9. Required heat exchanger surface area during take-off and cruise

realistic heat exchanger size, the required surface area during take-off must be reduced. This requires more efficient heat exchanger designs as well as an increase in the temperature difference between coolant and air. This is especially important to allow for hot day take-off scenarios. An ideal solution would be to increase the coolant temperature by using high temperature fuel cells, because no additional power and system components are required. Other possibilities include the use of a heat pump, i.e. a vapor cycle, to raise the coolant temperature or pre-coolers to reduce the air temperature before entering the heat exchanger. Both solutions come at the expense of additional system mass and complexity. Another possibility is to reduce the amount of fuel cell heat during take-off by increasing the number of propulsors to reduce the maximum power demand or via means of hybridisation.

The difference in required HX surface area during take-off and cruise leads to an oversized heat exchanger during cruise, increasing drag and reducing the benefit of the heat recovery of the ram jet effect. The goal of further research activities will be to expand the model scope, to optimize the whole propulsion system and to close the gap between required HX surface area during take-off and cruise.

3.3.2. Fan Area

In the calculation all cross sections are referenced via area ratios to the fan area, but how does the calculated fan area varies for the investigated load cases? Fig. 10 shows the reduction of the fan area with FPR. This due to the fact, that the jet velocity decreases with lower FPRs and as a consequence the rubberized engine increases in size to compensate with a higher mass flow to fulfil the thrust demand. Further is shown that for sizing at take-off conditions a maximum FPR exists. Because of the increase in air temperature during fan compression and the low coolant temperature, the temperature different

in the heat exchange can reaches zero, see Fig. 11. If the air and coolant temperature are equivalent an increase in heat exchange lengths is no more beneficial. This effect can be also seen in Fig. 9 where the HX surface area increases sharply due to the low temperate difference. To allow for higher FPRs during take-off it is necessary to increase the temperature difference by raising the coolant temperature or by lowering the air temperature. Sizing the heat propulsor under cruise conditions higher FPRs are possible because the ambient air temperature is much lower and thus higher compression ratios are possible wilt maintaining a positive temperature difference, see Fig. 11.
Due to the higher thrust demand the fan area at take-off is greater compared to cruise for the same FPR. For a more advanced design of the heat propulsor this difference will most likely be overcome by varying the FPR depending on the operating conditions. Adjustment of the FPR can be achieved with the help of variable fan pitch [12]. Coolant temperature and heat exchanger inlet area to fan area ratio have no significant impact on fan area as long as the temperature at the heat exchanger inlet allows for a positive temperature difference in the heat exchanger.
As a reference for state of the art turbofans, the engine of an A320neo has a fan area of about 3 m^2. This means that to achieve comparable fan areas high FPRs are required, but Fig. 5 shows that the total efficiency is higher for lower FPRs. As a consequence a trade off must be made between fan size and performance.

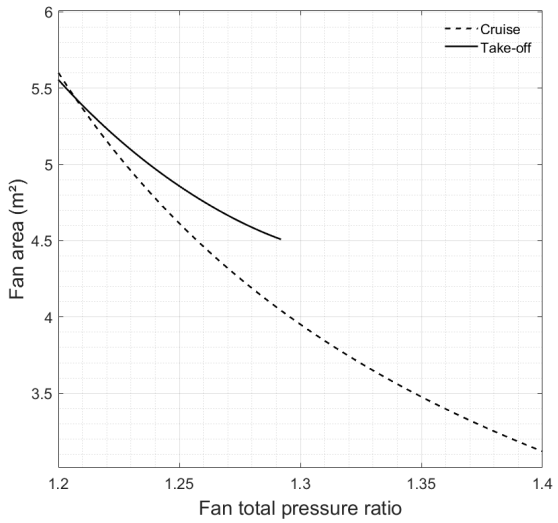

FIG. 10. Dependency of fan area on FPR

4. CONCLUSION

The integration of heat exchangers combined with a fan stage represents a promising approach to implement the thermal management system of fuel cell aircraft. The proposed layout not only overcomes the draw back of heat exchange induced drag in a high-speed flow regime but further offers the opportunity for enhanced performance and efficiency. The benefit of the final

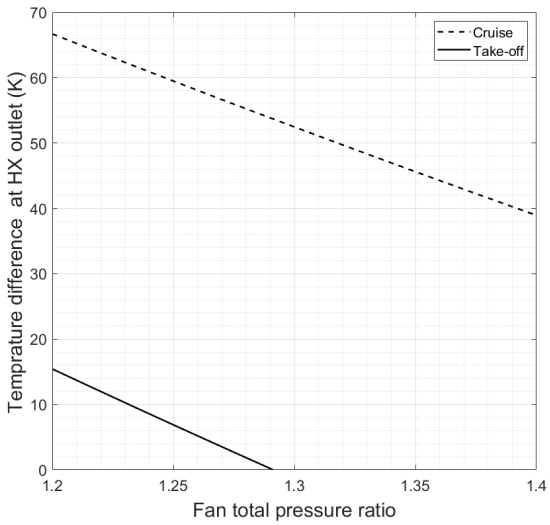

FIG. 11. Temperature difference of coolant and air at the heat exchanger outlet

heat propulsor design depends on the trade-off between heat propulsor size and heat exchanger pressure loss. As shown, a smaller but more efficient FPR requires larger diameters of the propulsor, therefore future studies should investigate the influence of the propulsor geometry on the external drag of the aircraft. This allows an efficient propulsor to be designed within reasonable dimensions.
The biggest challenge for the successful integration of the heat propulsor remains the discrepancy between take-off and cruise requirements. This problem is particularly difficult in case of high ambient temperatures (summer day in a desert region). The sizing of the heat exchanger for high ambient temperature at ground level leads to inefficiencies during cruise where the utilisation of the ram jet effect is most beneficial. The overall system architecture therefore must be improved to close the gap between the two load cases and to bring the necessary heat exchanger sizes closer together.
In future studies the model limits need to be extended and the degree of detail increased, in order to investigate the influence of the propulsor on aircraft design and to optimise the overall concept. Not only will detailed CFD be carried out, but the significance of the heat propulsor on aircraft mass, direct operating costs and life cycle costs will also be analysed.
It can be concluded, that by making use of the ram jet effect the heat propulsor promises significant advantages compared to non recuperating fuel cell propulsion systems.

Contact address:

matthias.ronovsky@tuwien.ac.at

References

[1] Majid Asli, Paul König, Dikshant Sharma, Evangelia Pontika, Jon Huete, Karunakar Reddy Konda, Ak-

ilan Mathiazhagan, Tianxiao Xie, Klaus Höschler, and Panagiotis Laskaridis. Thermal management challenges in hybrid-electric propulsion aircraft, 2024. DOI: 10.1016/j.paerosci.2023.100967.

[2] Stefan Kazula, Stefanie de Graaf, and Lars Enghardt. Review of fuel cell technologies and evaluation of their potential and challenges for electrified propulsion systems in commercial aviation, 2023. DOI: 10.33737/jgpps/158036.

[3] S. J. Miley. Aerodynamics of liquid-cooled aircraft engine installations. In *SAE Technical Papers*, 1985. DOI: 10.4271/850896.

[4] John V Becker and Donald D Baals. Analysis of heat and compressibility effects in internal flow systems and high-speed tests of a ram-jet system. *NACA*, NACA-TR-77, 1943.

[5] Chetan Kumar Sain, Jeffrey Hänsel, and Stefan Kazula. Preliminary Design of Air and Thermal Management of a Nacelle-Integrated Fuel Cell System for an Electric Regional Aircraft. In *2023 IEEE Transportation Electrification Conference and Expo, ITEC 2023*, 2023. DOI: 10.1109/ITEC55900.2023.10187105.

[6] International Organization for Standardization (ISO). Standard Atmosphere. Standard, Geneva, Switzerland, June 2018. ISO 2533:1979-12.

[7] D. Hintermayr and S. Kazula. Design and analysis of the air inlet system for fuel cell-powered electric propulsion systems in regional aircraft. *Deutscher Luft- und Raumfahrtkongress 2023*, Apr 2024. DOI: 10.25967/610194.

[8] Ramesh K Shah and Dusan P Sekulic. *Fundamentals of Heat Exchanger Design*. John Wiley Sons, Incorporated, 2023. ISBN: 1-119-88329-6.

[9] Jens Mischner, Hans-Burkhard Horlacher, and Ulf Helbig. *Fluiddynamische Berechnung von Hochdruckgasleitungen*. Springer Reference Technik, 2018. ISBN: 3662503549.

[10] Mark R. Nichols. Investigation of flow through an intercooler set at various angles to the supply duct. *NACA-WR-L-408*, Apr 1942.

[11] Dietrich Küchemann and Johanna Weber. *Aerodynamics of propulsion*. McGraw-Hill, 1953.

[12] Mavroudis D Kavvalos, Xin Zhao, Rainer Schnell, Ioanna Aslanidou, Anestis I Kalfas, and Konstantinos G Kyprianidis. A Modelling Approach of Variable Geometry for Low Pressure Ratio Fans. In *International Symposium on Air Breathing Engines*, 2019.